Doppler Resilient Complementary Sequences: Theoretical Bounds and Optimal Constructions

Bingsheng Shen, *Member, IEEE*, Yang Yang, *Member, IEEE*, Zhengchun Zhou, *Member, IEEE*, Zilong Liu, *Senior Member, IEEE*, Pingzhi Fan, *Fellow, IEEE*

***Abstract*—This paper studies Doppler resilient complementary sequences (DRCSs) whereby the ambiguity functions (AFs) of multiple element sequences are summed to attain low/zero AF values. We first derive a set of AF lower bounds for unimodular DRCS sets, which include the existing bounds on AFs as special cases. These bounds may be used as theoretical design guidelines to measure the optimality of DRCS sets against Doppler effect. In addition, we introduce some constructions of DRCS sets based on mathematical tools such as orthogonal matrices, circular Florentine rectangles and difference sets, which can generate the optimal DRCS set. Finally, we evaluate the feasibility of DRCSs for pulse train waveform design.**

***Index Terms*—Doppler resilient complementary sequence, ambiguity function, orthogonal matrices, theoretical bounds, Florentine rectangles, difference sets.**

I. Introduction

The concept of "complementary sequence (CS)" was introduced by Marcel J. E. Golay in the 1960s [1]. Formally, a pair of equal-length sequences is referred to as a Golay complementary pair (GCP) if the two constituent sequences have zero aperiodic auto-correlation sums for all the non-zero time-shifts. In this case, each constituent sequence is called a CS. In 1972, Tseng and Liu studied mutually orthogonal sets of CSs each consisting of two or more constituent sequences and any distinctive two having zero aperiodic cross-correlation sums for any time-shifts [2]. Later, Suehiro and Hatori proposed complete complementary codes, which are essentially mutually orthogonal sets of CSs with largest set size (i.e., equal to the number of constituent sequences) [3]. Inspired by Golay, Bomer *et al.* and Luke further investigated periodic CSs [4] and odd-periodic CSs [5], respectively.

Due to their ideal correlation properties, CSs have found numerous applications in, for example, channel estimation [6], Doppler resilient waveform design [7], [8], omnidirectional precoding for massive multiple-input multiple-output (MIMO) [9], preamble sequence development for grant-free non-orthogonal multiple access (NOMA) [10], spreading code design for asynchronous multicarrier code-division multiple-access (MC-CDMA) [11], [12], peak-to-average power ratio (PAPR) reduction in orthogonal frequency-division multiplexing (OFDM) [13], and integrated sensing and communication (ISAC) [14], [15], etc.

The maximum number of mutually orthogonal sets of CSs is upper bounded by the number of constituent sequences. This may not be satisfactory for some application scenarios (e.g., the aforementioned MC-CDMA systems). To address this issue, quasi-complementary sequence sets (QCSSs) having low correlation magnitude are studied [16]. In fact, the theoretical lower bound of QCSSs was studied as early as 1974, but Welch did not use the term "QCSS" at that time, instead it became "multichannel aperiodic correlation". This lower bound is as follows [17, Theorem (Multichannel Aperiodic Correlation)]:

$$\tilde{\theta}_{\max} \geq MN\sqrt{\frac{K/M-1}{K(2N-1)-1}}, \tag{1}$$

where $\tilde{\theta}_{\max}$, K, M, N denote the maximum aperiodic correlation magnitude, the set size, the number of constituent sequences, and the constituent sequence length, respectively. In 2011, Liu *et al.* obtained a number of lower bounds on the maximum correlation magnitude for aperiodic, periodic, and odd periodic QCSS [16]:

$$\tilde{\theta}_{\max} \geq MN\sqrt{\frac{(K/M-1)Z-N+1}{(KZ-1)(N+Z-1)}}, \tag{2}$$

$$\theta_{\max} = \hat{\theta}_{\max} \geq MN\sqrt{\frac{KZ-MN}{(KZ-1)MN}}, \tag{3}$$

where $\theta_{\max}$ and $\hat{\theta}_{\max}$ denote the maximum periodic and odd periodic correlation magnitude, respectively, Z is the correlation zone width. In 2014, Liu *et al.* extended the idea of Levenshtein bound and provided a tighter correlation lower bound for aperiodic QCSSs when $K \geq 3M$, $M \geq 2$ and $N \geq 2$ [18]:

$$\tilde{\theta}_{\max} \geq \sqrt{MN\left(1-2\sqrt{\frac{M}{3K}}\right)}. \tag{4}$$

Representative constructions on QCSSs with low correlation properties can be found in [19]–[24].

Modern communication and radar systems must deal with the notorious Doppler effect in high mobility environments. Conventional sequences including CSs may not work well in this case. New sequences highly robust to Doppler are expected. Such sequences are called Doppler resilient sequences (DRSs) [25]. Unlike the traditional sequence design theory,

B. Shen, Z. Zhou and P. Fan are with the School of Information Science and Technology, Southwest Jiaotong University, Chengdu, 611756, China. E-mail: bsshen9527@swjtu.edu.cn, zzc@swjtu.edu.cn, p.fan@ieee.org.

Y. Yang is with the School of Mathematics, Southwest Jiaotong University, Chengdu, 611756, China. E-mail: yang_data@swjtu.edu.cn.

Z. Liu is with the School of Computer Science and Electronic Engineering, University of Essex, CO4 3SQ Colchester, U.K. E-mail: zilong.liu@essex.ac.uk.

ambiguity function (AF) is defined to measure the receiver's response to both delay and Doppler shifts. In 2013, Ding *et al.* generalized the maximum periodic AF lower bound for DRS sets in [26]. DRS sets meeting the derived bound in [26] are not known. In 2022, Ye *et al.* improved the lower bound in [26] by utilizing the property that the auto-AF at zero delay in a unimodular sequence is equal to zero for any non-zero Doppler [25]. In addition, several DRS sets that can (or almost) meet their proposed periodic AF lower bound are developed.

Conventional CSs are defined based on correlation sums, but this may not guarantee low AF sidelobes [27]. In [7], Pezeshki *et al.* proposed a construction of Doppler resilient Golay complementary waveform (DRGCW) based GCPs and Prouhet-Thue-Morse (PTM) sequences. The core idea of DRGCW is to transmit a GCP several times over a pulse train according to the unique structure of a PTM sequence. In such a way, the Taylor expansion of its AF near zero Doppler exhibits high-order zeros, thus leading to Doppler-resilient AF. Tang *et al.* extended DRGCW to MIMO scenarios by leveraging complete complementary codes and generalized PTM sequences [28]. To improve the Doppler resilience of DRGCWs, Dang *et al.* adopted weighting of the receiving filter, albeit at the cost of compromised signal-to-noise ratio (SNR) [29]. A number of subsequent research works alongside this direction can also be found in [30]–[34]. It is worth noting that DRGCW assumes that the Doppler shift is significantly smaller than the pulse repetition frequency (PRF), or the pulse duration is much shorter than the pulse repetition interval (PRI). Based on this assumption, the Doppler shift inside the pulse can be ignored, and only the Doppler shift between different pulses needs to be considered [35]. In some cases, this assumption does not hold due to large Doppler shifts.

Inspired by CSs and DRSs, this paper aims to study DRCS sets, whereby the AF of a DRCS is characterized by the summation of AFs of all constituent sequences. The main contributions are summarized as follows:

- Theoretical AF lower bounds on unimodular DRCS sets with respect to the set size K, the number of constituent sequences M, the sequence length N, and the zone size $(-Z_x, Z_x) \times (-Z_y, Z_y)$ of low/zero ambiguity zone (LAZ/ZAZ) are derived. It is shown that our derived bounds include the existing ones as special cases. Additionally, our derived bounds also indicate that the DRCS can achieve thumbtack-shaped AFs across the global delay-Doppler area.
- To validate the concept of DRCSs and the above theoretical bounds, some constructions of DRCS sets are presented, using mathematical tools such as orthogonal matrices, Florentine rectangles and difference sets, which can generate the optimal DRCS set. The effectiveness of DRCS-based pulse train radar waveform in target detection is evaluated by simulation.

The structure of this paper is outlined as follows: In Section II, we introduce the essential mathematical tools and notations utilized in this work. In Section III, we aim to derive three types of lower bounds on DRCS sets. These bounds are tight in the sense that they can be achieved with equality by some optimal DRCS sets, which are presented in Section IV. Then, we verified the target detection capability of DRCS-based radar waveform in Section V. Lastly, Section VI concludes this paper.

Notation: $\xi_N = \exp(2\pi\sqrt{-1}/N)$ denotes the primitive N-th root of unity; $\mathbb{Z}_N = \{0, 1, \cdots, N-1\}$ denotes the set of all integers modulo N; x^* denotes the conjugate of the complex number x; $\lfloor x \rfloor$ denotes the largest integer less than x; $\odot$ denotes the Hadamard product.

II. Preliminaries

A. Doppler Resilient Complementary Sequence

A conventional sequence set $\boldsymbol{A}$ contains K sequences of length N, and each of which has all of its entries taking values from a set, called the alphabet. Namely, $\boldsymbol{A} = \{\boldsymbol{a}_0, \boldsymbol{a}_1, \cdots, \boldsymbol{a}_{K-1}\}$, $\boldsymbol{a}_k = (a_{k,0}, a_{k,1}, \cdots, a_{k,N-1})$, where $0 \le k < K$. In this paper, the alphabet of interest is the set of the complex roots of unity, i.e., unimodular sequence. For two sequence $\boldsymbol{a}_u$ and $\boldsymbol{a}_v$ in $\boldsymbol{A}$, their aperiodic cross-AF is defined as follows:

$$\widetilde{AF}_{\boldsymbol{a}_u,\boldsymbol{a}_v}(\tau, f) = \begin{cases} \sum_{i=0}^{N-1-\tau} a_{u,i} a_{v,i+\tau}^* \xi_N^{fi}, & 0 \le \tau < N; \\ \sum_{i=-\tau}^{N-1} a_{u,i} a_{v,i+\tau}^* \xi_N^{fi}, & -N < \tau < 0; \\ 0, & |\tau| \ge N. \end{cases} \tag{5}$$

Specially, the aperiodic cross AF shall become periodic/odd-periodic cross AF when the summation variable $t = 0$ to $N-1 \pmod N$, that is,

$$AF_{\boldsymbol{a}_u,\boldsymbol{a}_v}(\tau, f) = \sum_{i=0}^{N-1} a_{u,i} a_{v,i+\tau}^* \xi_N^{fi}, \tag{6}$$

$$\widehat{AF}_{\boldsymbol{a}_u,\boldsymbol{a}_v}(\tau, f) = \sum_{i=0}^{N-1} a_{u,i} a_{v,i+\tau}^* (-1)^{\lfloor \frac{i+\tau}{N} \rfloor} \xi_N^{fi}, \tag{7}$$

where τ and f are called delay- and Doppler- shifts, respectively, $|\tau|, |f| \in \mathbb{Z}_N$, and the summation $i + \tau$ is modulo N. If $u = v$, we call them auto-AF, and denoted by $\widetilde{AF}_{\boldsymbol{a}_u}(\tau, f)$, $AF_{\boldsymbol{a}_u}(\tau, f)$, $\widehat{AF}_{\boldsymbol{a}_u}(\tau, f)$, respectively.

An ideal ambiguity function could be depicted as a spike peaking at the origin and having a value of zero everywhere else. This type of ambiguity function offers perfect resolution between adjacent targets, regardless of their proximity to each other. Due to the limitations of the theoretical bounds, conventional sequences cannot realize the ideal ambiguity function [25], but the DRCS proposed in this paper can achieve it.

A DRCS set $\mathcal{C}$ contains K (i.e., set size) DRCSs, each DRCS consists of M (i.e., flock size) elementary sequences of length N. Namely, $\mathcal{C} = \{\boldsymbol{C}^{(0)}, \boldsymbol{C}^{(1)}, \cdots, \boldsymbol{C}^{(K-1)}\}$, $\boldsymbol{C}^{(k)} = \{\boldsymbol{c}_0^{(k)}, \boldsymbol{c}_1^{(k)}, \cdots, \boldsymbol{c}_{M-1}^{(k)}\}$, and $\boldsymbol{c}_m^{(k)} = (c_{m,0}^{(k)}, c_{m,1}^{(k)}, \cdots, c_{m,N-1}^{(k)})$, where $0 \le k < K$ and $0 \le m < M$. Therefore, it is helpful to write each

DRCS as a 2-D matrix by vertically stacking all of its indexed elementary sequences row by row, e.g.,

$$\boldsymbol{C}^{(k)} = \begin{bmatrix} \boldsymbol{c}_0^{(k)} \\ \boldsymbol{c}_1^{(k)} \\ \vdots \\ \boldsymbol{c}_{M-1}^{(k)} \end{bmatrix} = \begin{bmatrix} c_{0,0}^{(k)} & c_{0,1}^{(k)} & \cdots & c_{0,N-1}^{(k)} \\ c_{1,0}^{(k)} & c_{1,1}^{(k)} & \cdots & c_{1,N-1}^{(k)} \\ \vdots & \vdots & \ddots & \vdots \\ c_{M-1,0}^{(k)} & c_{M-1,1}^{(k)} & \cdots & c_{M-1,N-1}^{(k)} \end{bmatrix}. \quad (8)$$

For two DRCSs $\boldsymbol{C}^{(k_1)}$ and $\boldsymbol{C}^{(k_2)}$, their periodic cross-AF is defined as the periodic cross-AF sum, i.e.,

$$AF_{\boldsymbol{C}^{(k_1)},\boldsymbol{C}^{(k_2)}}(\tau, f) = \sum_{m=0}^{M-1} AF_{\boldsymbol{c}_m^{(k_1)},\boldsymbol{c}_m^{(k_2)}}(\tau, f), \quad (9)$$

when $k_1 = k_2 = k$, it is abbreviated to $AF_{\boldsymbol{C}^{(k)}}(\tau, f)$. Similarly, the aperiodic AF and odd-periodic AF of the DRCS are represented by $\widetilde{AF}$ and $\widehat{AF}$ respectively. This paper will focus on investigating periodic AF with the aid of certain mathematical tools.

Remark 1. Please note that although the concept of DRCSs is introduced in this paper, its idea was proposed by Turyn as early as 1963. In [36], Turyn studied the mean square value of the AF of binary DRCS containing two element sequences.

Given a low ambiguity zone (LAZ) $\Pi \subseteq (-N, N) \times (-N, N)$, the maximum periodic ambiguity magnitude of DRCS set $\mathcal{C}$ over a region Π is defined as $\theta_{\max} = \{\theta_a, \theta_c\}$, where the maximal periodic auto-ambiguity magnitude

$$\theta_a = \max\{|AF_{\boldsymbol{C}}(\tau, f)| : \boldsymbol{C} \in \mathcal{C}, (\tau, f) \neq (0, 0) \in \Pi\}, \quad (10)$$

and the maximal periodic cross-ambiguity magnitude

$$\theta_c = \max\{|AF_{\boldsymbol{C},\boldsymbol{D}}(\tau, f)| : \boldsymbol{C}, \boldsymbol{D} \in \mathcal{C}, (\tau, f) \in \Pi\}. \quad (11)$$

If $\theta_{\max} = 0$, the LAZ is called the zero ambiguity zone (ZAZ). Likewise, the symbols $\tilde{\theta}_{\max}$ and $\hat{\theta}_{\max}$ represent the maximum aperiodic and odd-periodic ambiguity amplitudes, respectively.

A DRCS set $\mathcal{C}$ with maximum ambiguity magnitude $\theta_{\max}$ over region Π is denoted by $(K, M, N, \theta_{\max}, \Pi)$-DRCS set. In addition, if we consider global AF with $\Pi = (-N, N) \times (-N, N)$, then $\mathcal{C}$ is denoted by $(K, M, N, \theta_{\max})$-DRCS set. Further, if $\theta_{\max} = 0$, then $\mathcal{C}$ is called a perfect DRCS set, denoted by (K, M, N)-DRCS set, and each one is called a perfect DRCS. In particular, the DRS set [25] can be seen as a special case of the DRCS set, where $M = 1$, denoted by $(K, N, \theta_{\max}, \Pi)$-DRS set.

B. Circular Florentine Rectangle

Definition 1. A Tuscan-k rectangle of size $r \times N$ has r rows and N columns such that

C1: each row is a permutation of the N symbols and

C2: for any two distinct symbols a and b and for each $1 \leq m \leq k$, there is at most one row in which b is m steps to the right of a.

When $k = N - 1$, it is called a Tuscan-$(N-1)$ rectangle or Florentine rectangle (FR). When the circularly-shifted versions of the rows of a Florentine rectangle satisfying the condition that b is $N - m$ steps to the right of a is equivalent to the fact that b is m steps to the left of a, it is called a circular FR (CFR).

For any integer $N > 0$, let $\tilde{F}(N)$ denote the largest integer such that CFR of size $\tilde{F}(N) \times N$ exists. Some known results of $\tilde{F}(N)$ are given in the following lemma [37].

Lemma 1. For $N \geq 2$, we have the following bounds for $\tilde{F}(N)$:

- $\tilde{F}(N) = 1$ when N is even,
- $p - 1 \leq \tilde{F}(N) \leq N - 1$, where p is the smallest prime factor of N,
- $\tilde{F}(N) = N - 1$ when N is a prime,
- $\tilde{F}(N) \leq N - 3$ when $N = 15 \pmod{18}$.

Lemma 2. Let N be a positive integer, and p is the smallest prime factor of N. Define a rectangle $\boldsymbol{F} = [f_{i,j}]$ of size $(p-1) \times N$, $f_{i,j} = (i+1) \times j \pmod{N}$, $0 \leq i < p-1$, $0 \leq j < N$, then $\boldsymbol{F}$ is a CFR.

Example 1. Let $N = 7$. According to Lemma 2, we can get a CFR of size 6×7 over $\mathbb{Z}_7$ as follows:

$$\boldsymbol{F} = \begin{bmatrix} 0 & 1 & 2 & 3 & 4 & 5 & 6 \\ 0 & 2 & 4 & 6 & 1 & 3 & 5 \\ 0 & 3 & 6 & 2 & 5 & 1 & 4 \\ 0 & 4 & 1 & 5 & 2 & 6 & 3 \\ 0 & 5 & 3 & 1 & 6 & 4 & 2 \\ 0 & 6 & 5 & 4 & 3 & 2 & 1 \end{bmatrix}. \quad (12)$$

To proceed, let us present the following lemmas which are useful for our subsequent proof.

Lemma 3. Let $\boldsymbol{F}$ be an $M \times N$ CFR over $\mathbb{Z}_N$. For $0 \leq i \neq j < M$, $f_{i,t} - f_{j,t+\tau \pmod{N}} = 0$ exactly has one solution for each $0 \leq \tau < N$, where $t \in [0, N)$.

Lemma 4. Let $\boldsymbol{F}$ be an $M \times N$ FR over $\mathbb{Z}_N$. For $0 \leq i \neq j < M$, $f_{i,t} - f_{j,t+\tau} = 0$ has at most one solution for each $0 \leq \tau < N$, where $t \in [0, N - \tau)$.

C. Difference Set

Definition 2. For any subset $\mathfrak{D} = \{d_0, d_1, \cdots, d_{M-1}\} \subseteq \mathbb{Z}_N$, the difference function of $\mathfrak{D}$ is defined as

$$d_{\mathfrak{D}}(\tau) = |(\tau + \mathfrak{D}) \cap \mathfrak{D}|, \ \tau \in \mathbb{Z}_N. \quad (13)$$

$\mathfrak{D}$ is said to be a (N, M, λ) difference set (DS) if and only if $d_{\mathfrak{D}}(\tau)$ takes on the value λ for $N - 1$ times when τ ranges over the nonzero elements of $\mathbb{Z}_N$.

For a (N, M, λ)-DS, obviously, we have $M(M-1) = (N-1)\lambda$. Moreover, we have the following lemma.

Lemma 5. For a (N, M, λ)-DS, $\tau \neq 0 \pmod{N}$, we have

$$\left| \sum_{m=0}^{M-1} \xi_N^{\tau d_m} \right| = \sqrt{M - \lambda} = \sqrt{\frac{M(N-M)}{N-1}}. \quad (14)$$

III. Bounds of DRCS Sets

For different ambiguity functions, this section will give the theoretical lower bound of maximum ambiguity magnitude of DRCS sets. Before giving the main theorem, we give the following lemma [25], which is helpful for the derivation of the theoretical lower bound.

Lemma 6. For any unimodular sequence $\boldsymbol{a}$, we have

$$|AF_{\boldsymbol{a}}(0,f)| = |\widetilde{AF}_{\boldsymbol{a}}(0,f)| = |\widehat{AF}_{\boldsymbol{a}}(0,f)| = 0 \tag{15}$$

for any $f \neq 0$.

A. Periodic Theoretical Bound of DRCS Set

In this subsection, we introduce our main theorem and provide a straightforward derivation by constructing a big matrix comprising all possible delay- and Doppler-shifted versions of complementary sequences.

Theorem 1. For a $(K, M, N, \theta_{\max}, \Pi)$-DRCS set, where LAZ $\Pi = (-Z_x, Z_x) \times (-Z_y, Z_y)$, $1 \leq Z_x, Z_y \leq N$, we have

$$\theta_{\max} \geq \frac{MN}{\sqrt{Z_y}} \sqrt{\frac{\frac{KZ_xZ_y}{MN} - 1}{KZ_x - 1}}. \tag{16}$$

Specially, if $\theta_{\max} = 0$, it reduces to

$$K \leq \frac{MN}{Z_xZ_y}. \tag{17}$$

Proof. Let us construct a matrix $\boldsymbol{H}$ of size $KZ_xZ_y \times MN$, which is expressed as

$$\boldsymbol{H} = \begin{bmatrix} \boldsymbol{H}^{(0)} \\ \boldsymbol{H}^{(1)} \\ \vdots \\ \boldsymbol{H}^{(Z_y-1)} \end{bmatrix}. \tag{18}$$

For $\boldsymbol{H}^{(y)}$, its $(kZ_x + \lambda)$-th row is

$$\begin{aligned} \boldsymbol{h}^{(y)}_{kZ_x+\lambda} = \Big[&T(\boldsymbol{c}^{(k)}_0, \lambda) \odot \boldsymbol{p}_y, T(\boldsymbol{c}^{(k)}_1, \lambda) \odot \boldsymbol{p}_y, \\ &\cdots, T(\boldsymbol{c}^{(k)}_{M-1}, \lambda) \odot \boldsymbol{p}_y\Big], \end{aligned} \tag{19}$$

where $0 \leq k < K$, $0 \leq \lambda < Z_x$, $\boldsymbol{p}_y = (\xi_N^{0\times y}, \xi_N^{1\times y}, \cdots, \xi_N^{(N-1)\times y})$, and

$$\begin{aligned} T(\boldsymbol{a}^{(k)}_m, \lambda) = \Big(&a^{(k)}_{m,\lambda}, a^{(k)}_{m,\lambda+1}, \cdots, a^{(k)}_{m,N-1}, \\ &a^{(k)}_{m,0}, a^{(k)}_{m,1}, \cdots, a^{(k)}_{m,\lambda-1}\Big) \end{aligned} \tag{20}$$

represents periodic cyclic shift. It is not difficult to find that the inner product of $\boldsymbol{h}^{(y_1)}_{k_1Z_x+\lambda_1}$ and $\boldsymbol{h}^{(y_2)}_{k_2Z_x+\lambda_2}$ can be expressed as the AF between $\boldsymbol{C}^{(k_1)}$ and $\boldsymbol{C}^{(k_2)}$, or more precisely,

$$\left\langle \boldsymbol{h}^{(y_1)}_{k_1Z_x+\lambda_1}, \boldsymbol{h}^{(y_2)}_{k_2Z_x+\lambda_2} \right\rangle = AF_{\boldsymbol{C}^{(k_1)},\boldsymbol{C}^{(k_2)}}(\lambda_2 - \lambda_1, y_1 - y_2). \tag{21}$$

Therefore,

$$\begin{aligned} ||\boldsymbol{H}\boldsymbol{H}^{\mathrm{H}}||_F^2 = &\sum_{k=0}^{K-1} \sum_{\tau=1-Z_x}^{Z_x-1} \sum_{f=1-Z_y}^{Z_y-1} (Z_x - |\tau|) \\ &\times (Z_y - |f|)|AF_{\boldsymbol{C}^{(k)}}(\tau, f)|^2 \\ &+ \sum_{\substack{k_1,k_2=0 \\ k_1\neq k_2}}^{K-1} \sum_{\tau=1-Z_x}^{Z_x-1} \sum_{f=1-Z_y}^{Z_y-1} (Z_x - |\tau|) \\ &\times (Z_y - |f|)|AF_{\boldsymbol{C}^{(k_1)},\boldsymbol{C}^{(k_2)}}(\tau, f)|^2. \end{aligned} \tag{22}$$

Based on Lemma 6, we have

$$\sum_{k=0}^{K-1} \sum_{f=1-Z_y}^{Z_y-1} Z_x(Z_y - |f|)|AF_{\boldsymbol{C}^{(k)}}(0,f)|^2 = KZ_xZ_y(MN)^2. \tag{23}$$

Further, we obtain

$$\begin{aligned} &||\boldsymbol{H}\boldsymbol{H}^{\mathrm{H}}||_F^2 \\ &\leq KZ_xZ_y(MN)^2 + KZ_x(Z_x-1)Z_y^2\theta_a^2 \\ &\quad + K(K-1)Z_x^2Z_y^2\theta_c^2 \\ &\leq KZ_xZ_y(MN)^2 + KZ_xZ_y^2(KZ_x-1)\theta_{\max}^2. \end{aligned} \tag{24}$$

On the other hand, $||\boldsymbol{H}^{\mathrm{H}}\boldsymbol{H}||_F^2 \geq MN(KZ_xZ_y)^2$. Because $||\boldsymbol{H}\boldsymbol{H}^{\mathrm{H}}||_F^2 = ||\boldsymbol{H}^{\mathrm{H}}\boldsymbol{H}||_F^2$, we have

$$\begin{aligned} MN(KZ_xZ_y)^2 \leq &KZ_xZ_y(MN)^2 \\ &+ KZ_xZ_y^2(KZ_x-1)\theta_{\max}^2. \end{aligned} \tag{25}$$

The result then follows. □

Remark 2. As a special case, certain known bounds can be derived from Theorem 1. When $M = 1$, Theorem 1 reduces to the Ye-Zhou-Fan-Liu-Lei-Tang bound for DRS sets in [25]. When $Z_y = 1$, Theorem 1 reduces to the Liu-Guan-Ng-Chen bound for low correlation zone complementary sequence (LCZ-CS) sets in [16].

According to Theorem 1, the following corollary can also be derived.

Corollary 1. With the same notations as Theorem 1. When $Z_x = Z_y = N$, a lower bound of global ambiguity is given as

$$\theta_{\max} \geq M\sqrt{N}\sqrt{\frac{KN/M - 1}{KN - 1}}. \tag{26}$$

In particular, if $\theta_{\max} = 0$, we have

$$K \leq \frac{M}{N}, \tag{27}$$

which means that it is impossible to find two perfect DRCSs to achieve the zero cross-AF when $M \leq N < 2M$. In addition, we can get the Sarwate bound [38] of DRCS sets as follows

$$\frac{N-1}{MN(KN-M)}\theta_a^2 + \frac{K-1}{M(KN-M)}\theta_c^2 \geq 1. \tag{28}$$

B. Odd-Periodic Theoretical Bound of DRCS Set

In [39], Pursley highlighted the significance of odd-periodic correlations in digital signal processing. Generally, the same scenarios that apply to periodic sequences apply to odd-periodic sequences. This subsection will give the odd-periodic theoretical bound of the DRCS set.

Theorem 2. For a $(K, M, N, \hat{\theta}_{\max}, \Pi)$-DRCS set, where LAZ $\Pi = (-Z_x, Z_x) \times (-Z_y, Z_y)$, $1 \leq Z_x, Z_y \leq N$, we have

$$\hat{\theta}_{\max} \geq \frac{MN}{\sqrt{Z_y}} \sqrt{\frac{\frac{KZ_xZ_y}{MN} - 1}{KZ_x - 1}}. \tag{29}$$

Proof. Construct a 'big" matrix $\hat{\boldsymbol{H}}$ through odd-periodic cyclic shifts, that is,

$$\hat{\boldsymbol{h}}_{kZ_x+\lambda}^{(y)} = \Big[\hat{T}(\boldsymbol{c}_0^{(k)},\lambda)\odot\boldsymbol{p}_y, \hat{T}(\boldsymbol{c}_1^{(k)},\lambda)\odot\boldsymbol{p}_y, \cdots, \hat{T}(\boldsymbol{c}_{M-1}^{(k)},\lambda)\odot\boldsymbol{p}_y\Big], \quad (30)$$

where

$$\hat{T}(\boldsymbol{a}_m^{(k)},\lambda) = \Big(a_{m,\lambda}^{(k)}, a_{m,\lambda+1}^{(k)}, \cdots, a_{m,N-1}^{(k)}, -a_{m,0}^{(k)}, -a_{m,1}^{(k)}, \cdots, -a_{m,\lambda-1}^{(k)}\Big) \quad (31)$$

represents odd-periodic cyclic shift. The rest of the proof is exactly the same as Theorem 1. □

Remark 3. Obviously, the right-hand sides of (16) and (29) are the same. In particular, when N is odd, a DRCS set satisfying (16) also satisfies (29) after the even-odd transformation [40].

In [25], Ye *et al.* provided lower bounds for the maximum ambiguity magnitude of periodic DRS sets and aperiodic DRS sets, but the case of odd-periodic was not given. Based on Theorem 2, we have the following corollary.

Corollary 2. For a $(K,N,\hat{\theta}_{\max},\Pi)$-DRS set, where LAZ $\Pi = (-Z_x,Z_x)\times(-Z_y,Z_y)$, $1\le Z_x,Z_y\le N$, then its maximum odd-periodic ambiguity magnitude is lower bounded by

$$\hat{\theta}_{\max} \ge \frac{N}{\sqrt{Z_y}}\sqrt{\frac{\frac{KZ_xZ_y}{N}-1}{KZ_x-1}}. \quad (32)$$

C. Aperiodic Theoretical Bound of DRCS Set

In this subsection, we will give the aperiodic theoretical bound of DRCS sets, which is similar to Theorem 1. The key point is to replace the right side of (19) with

$$T\Big([\boldsymbol{c}_0^{(k)}\odot\boldsymbol{p}_y,\boldsymbol{0}_{Z_x-1},\boldsymbol{c}_1^{(k)}\odot\boldsymbol{p}_y,\boldsymbol{0}_{Z_x-1},\cdots,\boldsymbol{c}_{M-1}^{(k)}\odot\boldsymbol{p}_y,\boldsymbol{0}_{Z_x-1}],\lambda\Big) \quad (33)$$

in the derivation, where $\boldsymbol{0}_{Z_x-1}$ is all-0 sequence of length Z_x-1.

Theorem 3. For a $(K,M,N,\tilde{\theta}_{\max},\Pi)$-DRCS set, where LAZ $\Pi = (-Z_x,Z_x)\times(-Z_y,Z_y)$, $1\le Z_x,Z_y\le N$, we have

$$\tilde{\theta}_{\max} \ge \frac{MN}{\sqrt{Z_y}}\sqrt{\frac{\frac{KZ_xZ_y}{M(N+Z_x-1)}-1}{KZ_x-1}}. \quad (34)$$

Theorem 3 is directly obtained through Theorem 1, and it can be further improved, especially when $\tilde{\theta}_{\max}=0$. Below, we will give a tighter aperiodic theoretical bound for the aperiodic DRCS set when $\tilde{\theta}_{\max}=0$.

Theorem 4. For an aperiodic $(K,M,N,\tilde{\theta}_{\max},\Pi)$-DRCS set, where ZAZ $\Pi=(-Z_x,Z_x)\times(-Z_y,Z_y)$, $1\le Z_x,Z_y\le N$, if $\tilde{\theta}_{\max}=0$, we have

$$K \le \frac{MN}{Z_xZ_y}. \quad (35)$$

The AF is a two-dimensional correlation function, it becomes a traditional correlation function when $f=0$. In this case, the DRCS set degenerates into the CS set, and its parameter is expressed as $(K,M,N,\tilde{\theta}_{\max},Z)$, where $Z\in[1,N]$ represents the low correlation zone (LCZ) width. In particular, if $\tilde{\theta}_{\max}=0$, the LCZ is called a zero correlation zone (ZCZ). The following restriction exist among the parameters of the CS set with ZCZ [41].

Lemma 7. For an aperiodic $(K,M,N,0,Z)$-CS set, we have $K\le MN/Z$.

Next, we will prove Theorem 4.

Proof. Let $\mathcal{C}=\{\boldsymbol{C}^{(0)},\boldsymbol{C}^{(1)},\cdots,\boldsymbol{C}^{(K-1)}\}$ be an aperiodic $(K,M,N,\tilde{\theta}_{\max}=0,\Pi)$-DRCS set, where LAZ $\Pi=(-Z_x,Z_x)\times(-Z_y,Z_y)$, $1\le Z_x,Z_y\le N$. Let us construct a matrix $\boldsymbol{C}^{(k,y)}$ of size $M\times N$, such that the m-th row of $\boldsymbol{C}^{(k,y)}$ is

$$\boldsymbol{c}_m^{(k,y)} = \boldsymbol{c}_m^{(k)}\odot\boldsymbol{p}_y, \quad (36)$$

where $\boldsymbol{p}_y$ is shown in (19). Because $\boldsymbol{C}^{(k)}$ is a DRCS with ZAZ Π, so is $\boldsymbol{C}^{(k,y)}$ is a CS with ZCZ width Z_x and $\{\boldsymbol{C}^{(k,y)}: 0\le k\le K-1, 0\le y\le Z_y-1\}$ is a $(KZ_y,M,N,0,Z_x)$-CS set. According to Lemma 7, we have

$$KZ_y \le MN/Z_x. \quad (37)$$

The result then follows. □

IV. Constructions of DRCS Sets

In the previous section, the relevant theoretical bounds of the DRCS sets were derived. This section will construct the DRCS set that can reach the theoretical bounds (that is, the parameters of the DRCS set can make the equality sign in the theoretical bounds hold, also known as optimal) based on some mathematical tools.

A. DRCS Sets Based on Orthogonal Matrices

Before giving the first construction, we first give the following theorem about perfect DRCS.

Theorem 5. Let $N\ge 2$ be an integer, and $\boldsymbol{b}=(b_0,b_1,\cdots,b_{N-1})$ be a random unimodular sequence. Define a DRCS $\boldsymbol{A}=\{\boldsymbol{a}_0,\boldsymbol{a}_1,\cdots,\boldsymbol{a}_{N-1}\}$, each $\boldsymbol{a}_m=(a_{m,0},a_{m,1},\cdots,a_{m,N-1})$, and

$$a_{m,n} = b_n\xi_N^{mn}, \quad (38)$$

where $0\le m<N$, $0\le n<N$. Then $\boldsymbol{A}$ is a perfect aperiodic DRCS.

Proof. For any $(\tau,f)\ne(0,0)$, since $\boldsymbol{b}$ is a random unimodular sequence, then we have

$$\begin{aligned}\widetilde{AF}_{\boldsymbol{A}}(\tau,f) &= \sum_{m=0}^{N-1}\sum_{i=0}^{N-1-\tau} a_{m,i}a_{m,i+\tau}^*\xi_N^{if}\\ &= \sum_{i=0}^{N-1-\tau} b_ib_{i+\tau}^*\xi_N^{if}\sum_{m=0}^{N-1}\xi_N^{-m\tau}\\ &= 0.\end{aligned} \quad (39)$$

Therefore, $\boldsymbol{A}$ is a perfect aperiodic DRCS. □

Based on Theorem 5, we propose the following construction of perfect DRCS sets.

Theorem 6. Let $\boldsymbol{A}=\{\boldsymbol{a}_0,\boldsymbol{a}_1,\cdots,\boldsymbol{a}_{N-1}\}$ be a perfect DRCS of size N and of length N as shown in Theorem 5, and $\boldsymbol{O}=\{o_{i,j}\}_{i,j=0}^{P-1}$ be a orthogonal matrix of order P, where $|o_{i,j}|=1$. Define a DRCS set $\mathcal{A}=\{\boldsymbol{A}^{(0)},\boldsymbol{A}^{(1)},\cdots,\boldsymbol{A}^{(P-1)}\}$, each $\boldsymbol{A}^{(k)}=\{\boldsymbol{a}_0^{(k)},\boldsymbol{a}_1^{(k)},\cdots,\boldsymbol{a}_{PN-1}^{(k)}\}$, and $\boldsymbol{a}_{rN+u}^{(k)}=o_{k,r}\boldsymbol{a}_u$, where $0\le r,k<P$, $0\le u<N$. Then $\mathcal{A}$ is a perfect aperiodic DRCS set.

Proof. Since $\boldsymbol{A}$ is a perfect DRCS, so is $\boldsymbol{A}^{(k)}$ for $0\le k<P$. For $0\le s\ne t<P$, we have

$$\begin{aligned}\widetilde{AF}_{\boldsymbol{A}^{(s)},\boldsymbol{A}^{(t)}}(\tau,f)&=\sum_{m=0}^{PN-1}\widetilde{AF}_{\boldsymbol{a}_m^{(s)},\boldsymbol{a}_m^{(t)}}(\tau,f)\\&=\sum_{r=0}^{P-1}\sum_{u=0}^{N-1}o_{s,r}o_{t,r}^{*}\widetilde{AF}_{\boldsymbol{a}_u,\boldsymbol{a}_u}(\tau,f)\\&=0.\end{aligned}\tag{40}$$

Therefore, $\mathcal{A}$ is a perfect aperiodic DRCS set. □

Remark 4. For two DRCSs $\boldsymbol{A}$ and $\boldsymbol{B}$, according to the definition, we have

$$AF_{\boldsymbol{A},\boldsymbol{B}}(\tau,f)=\widetilde{AF}_{\boldsymbol{A},\boldsymbol{B}}(\tau,f)+\widetilde{AF}^{*}_{\boldsymbol{B},\boldsymbol{A}}(N-\tau,f),\tag{41}$$

$$\widehat{AF}_{\boldsymbol{A},\boldsymbol{B}}(\tau,f)=\widetilde{AF}_{\boldsymbol{A},\boldsymbol{B}}(\tau,f)-\widetilde{AF}^{*}_{\boldsymbol{B},\boldsymbol{A}}(N-\tau,f),\tag{42}$$

which implies that the $\mathcal{A}$ obtained from Theorem 6 is also a perfect periodic/odd-periodic DRCS set.

Remark 5. The parameters of the perfect DRCS set generated by Theorem 6 is (P,PN,N), which can make the equal sign of (27) and (35) hold, so it is the optimal.

B. DRCS Sets Based on Circular Florentine Rectangles

In Theorem 6, as the set size increases, the flock size will also increase. This is not what we want because flock size usually represents time domain or frequency domain resources. To avoid increasing the flock size, the maximum ambiguity magnitude can be relaxed, leading to our next theorems, which is about the periodic DRCS set.

Theorem 7. For any positive integer $N\ge 2$, let $K=\tilde{F}(N)$ and $\boldsymbol{F}$ be a CFR of size $K\times N$ over $\mathbb{Z}_N$. For each $0\le k<K$, define a DRCS $\boldsymbol{C}^{(k)}=\{\boldsymbol{c}_0^{(k)},\boldsymbol{c}_1^{(k)},\cdots,\boldsymbol{c}_{N-1}^{(k)}\}$, where $\boldsymbol{c}_m^{(k)}=(c_{m,0}^{(k)},c_{m,1}^{(k)},\cdots,c_{m,N-1}^{(k)})$, and

$$c_{m,n}^{(k)}=\xi_N^{m\times f_{k,n}}\tag{43}$$

for $0\le m<N$, $0\le n<N$, $f_{k,n}$ is (k,n)-th element of $\boldsymbol{F}$. Then $\mathcal{C}=\{\boldsymbol{C}^{(k)}:0\le k<K\}$ is a periodic (K,N,N,N)-DRCS set.

Proof. For any $0\le k<K$, and $(\tau,f)\ne(0,0)$, we have

$$\begin{aligned}AF_{\boldsymbol{C}^{(k)}}(\tau,f)&=\sum_{m=0}^{N-1}\sum_{i=0}^{N-1}\xi_N^{m(f_{k,i}-f_{k,i+\tau})}\xi_N^{if}\\&=\sum_{i=0}^{N-1}\xi_N^{if}\sum_{m=0}^{N-1}\xi_N^{m(f_{k,i}-f_{k,i+\tau})}\\&=0,\end{aligned}\tag{44}$$

which means that $\boldsymbol{C}^{(k)}$ is a perfect periodic DRCS. Now consider the cross-AF of $\boldsymbol{C}^{(s)}$ and $\boldsymbol{C}^{(t)}$ for $0\le s\ne t<K$. In this case, we have

$$AF_{\boldsymbol{C}^{(s)},\boldsymbol{C}^{(t)}}(\tau,f)=\sum_{m=0}^{N-1}\sum_{i=0}^{N-1}\xi_N^{m(f_{s,i}-f_{t,i+\tau})}\xi_N^{if}.\tag{45}$$

According to Lemma 3, $f_{s,i}-f_{t,i+\tau}=0$ for $0\le i\le i+\tau<N$, $0\le s\ne t<K$, has one solution. Suppose this solution is i', we have

$$\begin{aligned}AF_{\boldsymbol{C}^{(s)},\boldsymbol{C}^{(t)}}(\tau,f)&=\sum_{m=0}^{N-1}\sum_{i=0}^{N-1}\xi_N^{m(f_{s,i}-f_{t,i+\tau})}\xi_N^{if}\\&=\xi_N^{i'f}N+\sum_{m=0}^{N-1}\sum_{i=0,i\ne i'}^{N-1}\xi_N^{m(f_{s,i}-f_{t,i+\tau})}\xi_N^{if}\\&=\xi_N^{i'f}N.\end{aligned}\tag{46}$$

Therefore, $|AF_{\boldsymbol{C}^{(s)},\boldsymbol{C}^{(t)}}(\tau,f)|=N$ for all $s\ne t$, $0\le\tau,f<N$. This completes the proof. □

Remark 6. For a periodic $(K,M,N,\theta_{\max},\Pi)$-DRCS set $\mathcal{C}$, where LAZ $\Pi=(-Z_x,Z_x)\times(-Z_y,Z_y)$, $1\le Z_x,Z_y\le N$, define the optimal factor ρ [19] as

$$\rho=\frac{\theta_{\max}}{\frac{MN}{\sqrt{Z_y}}\sqrt{\frac{\frac{KZ_xZ_y}{MN}-1}{KZ_x-1}}},\tag{47}$$

which is a measure of optimality. Obviously, $\rho\ge 1$ and $\mathcal{C}$ is optimal when $\rho=1$. For the DRCS set generated by Theorem 7, its optimal factor is

$$\rho=\frac{N}{N\sqrt{\frac{\tilde{F}(N)N-N}{\tilde{F}(N)N-1}}}.\tag{48}$$

Since $\lim\limits_{p\to\infty}\tilde{F}(N)=\infty$, so $\lim\limits_{p\to\infty}\rho=1$, where p is minimum prime factor of N. Hence, the DRCS set generated by Theorem 7 is asymptotically optimal. The optimal factor when N is a prime is shown in Table I.

Remark 7. Since each DRCS in Theorem 7 is a perfect DRCS, then $\theta_a=0$ and $\theta_c=N$. Furthermore,

$$\frac{N-1}{MN(KN-M)}\theta_a^2+\frac{K-1}{M(KN-M)}\theta_c^2=1\tag{49}$$

when N is a prime, $M=N$ and $K=\tilde{F}(N)=N-1$. This means that the DRCS set obtained by Theorem 7 is strictly optimal for the Sarwate bound in (28).

Example 2. Let $N=11$, and

$$\boldsymbol{F}=\begin{bmatrix}0&1&2&3&4&5&6&7&8&9&10\\0&2&4&6&8&10&1&3&5&7&9\\0&3&6&9&1&4&7&10&2&5&8\\0&4&8&1&5&9&2&6&10&3&7\\0&5&10&4&9&3&8&2&7&1&6\\0&6&1&7&2&8&3&9&4&10&5\\0&7&3&10&6&2&9&5&1&8&4\\0&8&5&2&10&7&4&1&9&6&3\\0&9&7&5&3&1&10&8&6&4&2\\0&10&9&8&7&6&5&4&3&2&1\end{bmatrix}\tag{50}$$

TABLE I: The optimal factor of DRCS sets generated by Theorem 7

Sequence length N	5	7	11	13	17	19	23	29	31	37	41
Optimal factor ρ	1.1255	1.0823	1.0493	1.0411	1.0309	1.0275	1.0225	1.0177	1.0165	1.0138	1.0124
Sequence length N	43	47	53	59	61	67	71	73	79	83	89
Optimal factor ρ	1.0118	1.0108	1.0096	1.0086	1.0083	1.0075	1.0071	1.0069	1.0064	1.0061	1.0057

TABLE II: The DRCS set $\mathcal{C}$ in Example 2

$\boldsymbol{C}^{(0)}$	$\boldsymbol{C}^{(1)}$	$\boldsymbol{C}^{(2)}$	$\boldsymbol{C}^{(3)}$	$\boldsymbol{C}^{(4)}$
$\begin{bmatrix}00000000000\\0123456789\bar{0}\\02468\bar{0}13579\\0369147\bar{0}258\\04815926\bar{0}37\\05\bar{0}49382716\\061728394\bar{0}5\\073\bar{0}6295184\\0852\bar{0}741963\\097531\bar{0}8642\\0\bar{0}987654321\end{bmatrix}$	$\begin{bmatrix}00000000000\\02468\bar{0}13579\\04815926\bar{0}37\\061728394\bar{0}5\\0852\bar{0}741963\\0\bar{0}987654321\\0123456789\bar{0}\\0369147\bar{0}258\\05\bar{0}49382716\\073\bar{0}6295184\\097531\bar{0}8642\end{bmatrix}$	$\begin{bmatrix}00000000000\\0369147\bar{0}258\\061728394\bar{0}5\\097531\bar{0}8642\\0123456789\bar{0}\\04815926\bar{0}37\\073\bar{0}6295184\\0\bar{0}987654321\\02468\bar{0}13579\\05\bar{0}49382716\\0852\bar{0}741963\end{bmatrix}$	$\begin{bmatrix}00000000000\\04815926\bar{0}37\\0852\bar{0}741963\\0123456789\bar{0}\\05\bar{0}49382716\\097531\bar{0}8642\\02468\bar{0}13579\\061728394\bar{0}5\\0\bar{0}987654321\\0369147\bar{0}258\\073\bar{0}6295184\end{bmatrix}$	$\begin{bmatrix}00000000000\\05\bar{0}49382716\\0\bar{0}987654321\\04815926\bar{0}37\\097531\bar{0}8642\\0369147\bar{0}258\\0852\bar{0}741963\\02468\bar{0}13579\\073\bar{0}6295184\\0123456789\bar{0}\\061728394\bar{0}5\end{bmatrix}$
$\boldsymbol{C}^{(5)}$	$\boldsymbol{C}^{(6)}$	$\boldsymbol{C}^{(7)}$	$\boldsymbol{C}^{(8)}$	$\boldsymbol{C}^{(9)}$
$\begin{bmatrix}00000000000\\061728394\bar{0}5\\0123456789\bar{0}\\073\bar{0}6295184\\02468\bar{0}13579\\0852\bar{0}741963\\0369147\bar{0}258\\097531\bar{0}8642\\04815926\bar{0}37\\0\bar{0}987654321\\05\bar{0}49382716\end{bmatrix}$	$\begin{bmatrix}00000000000\\073\bar{0}6295184\\0369147\bar{0}258\\0\bar{0}987654321\\061728394\bar{0}5\\02468\bar{0}13579\\097531\bar{0}8642\\05\bar{0}49382716\\0123456789\bar{0}\\0852\bar{0}741963\\04815926\bar{0}37\end{bmatrix}$	$\begin{bmatrix}00000000000\\0852\bar{0}741963\\05\bar{0}49382716\\02468\bar{0}13579\\0\bar{0}987654321\\073\bar{0}6295184\\04815926\bar{0}37\\0123456789\bar{0}\\097531\bar{0}8642\\061728394\bar{0}5\\0369147\bar{0}258\end{bmatrix}$	$\begin{bmatrix}00000000000\\097531\bar{0}8642\\073\bar{0}6295184\\05\bar{0}49382716\\0369147\bar{0}258\\0123456789\bar{0}\\0\bar{0}987654321\\0852\bar{0}741963\\061728394\bar{0}5\\04815926\bar{0}37\\02468\bar{0}13579\end{bmatrix}$	$\begin{bmatrix}00000000000\\0\bar{0}987654321\\097531\bar{0}8642\\0852\bar{0}741963\\073\bar{0}6295184\\061728394\bar{0}5\\05\bar{0}49382716\\04815926\bar{0}37\\0369147\bar{0}258\\02468\bar{0}13579\\0123456789\bar{0}\end{bmatrix}$

be a CFR of size 10×11 from Lemma 2. Based on Theorem 7, we get a DRCS set $\mathcal{C}$ as shown in Table I, where each element represents a power of ξ_{11} and "$\bar{0}$" is recorded as 10. The auto-AF and cross-AF of $\boldsymbol{C}^{(0)}$ and $\boldsymbol{C}^{(5)}$ are shown in Fig. 1.

According to the proof of Theorem 7 and Lemma 4, the following aperiodic DRCS set can be obtained.

Corollary 3. With the same notations as Theorem 7. If $\boldsymbol{F}$ is a FR of size $K \times N$, then $\mathcal{C}$ is an aperiodic (K, N, N, N)-DRCS set.

Remark 8. Compared with CFR, FR has a wider range of parameters, please see [23]. The current best situation is that when $\tilde{N}$ is a prime, there is a FR of size $N \times N$, where $N = \tilde{N} - 1$. In this case, the optimal factor of the aperiodic DRCS set obtained by Corollary 3 is

$$\tilde{\rho} = \frac{\tilde{\theta}_{\max}}{\frac{MN}{\sqrt{Z_y}}\sqrt{\frac{\frac{KZ_xZ_y}{M(N+Z_x-1)}-1}{KZ_x-1}}} = \sqrt{2},\ \ N \to \infty, \tag{51}$$

where $\tilde{\theta}_{\max} = K = M = Z_x = Z_y = N$. Liu *et al.* [19] referred to the situation of $1 < \tilde{\rho} < 2$ near optimal.

C. DRCS Sets Based on Difference Sets

The Theorem 7 provides a framework for constructing optimal DRCS set using circular Florentine rectangles. In order to obtain more DRCS sets, this subsection will propose another framework based on difference sets.

Theorem 8. Let $\mathfrak{D} = \{d_0, d_1, \cdots, d_{M-1}\}$ be a (N, M, λ)-DS, $\boldsymbol{S} = \{\boldsymbol{s}_0, \boldsymbol{s}_1, \cdots, \boldsymbol{s}_{K-1}\}$ be a $(K, N, \alpha_{\max}, \Pi)$-DRS set, where $\Pi = (-Z_x, Z_x) \times (-Z_y, Z_y)$. Define a DRCS set $\mathcal{C} = \{\boldsymbol{C}^{(k)} : 0 \le k \le K-1\}$, $\boldsymbol{C}^{(k)} = \{\boldsymbol{c}_0^{(k)}, \boldsymbol{c}_1^{(k)}, \cdots, \boldsymbol{c}_{M-1}^{(k)}\}$, $\boldsymbol{c}_m^{(k)} = (c_{m,0}^{(k)}, c_{m,1}^{(k)}, \cdots, c_{m,N-1}^{(k)})$, and

$$c_{m,n}^{(k)} = s_{k,n} \times \xi_N^{nd_m}, \tag{52}$$

where $0 \le k < K-1$, $0 \le m < M$, and $0 \le n < N$. Then $\mathcal{C}$ is a periodic $(K, M, N, \theta_{\max}, \Pi)$-DRCS set, where $\theta_{\max} = \max\{\theta_{\tau \ne 0}, \theta_{\tau = 0}\}$, and

$$\theta_{\tau \ne 0} = \alpha_{\max}\sqrt{\frac{M(N-M)}{N-1}}, \tag{53}$$

$$\theta_{\tau = 0} = M \cdot \max_{k_1 \ne k_2} |AF_{\boldsymbol{s}_{k_1}, \boldsymbol{s}_{k_2}}(0, f)|. \tag{54}$$

Proof. For $0 \le k_1, k_2 \le K-1$, we have

$$\begin{aligned} AF_{\boldsymbol{C}^{(k_1)}, \boldsymbol{C}^{(k_2)}}(\tau, f) &= \sum_{m=0}^{M-1} \xi_N^{-\tau d_m} \sum_{i=0}^{N-1} s_{k_1,i} s_{k_2,i+\tau}^* \xi_N^{if} \\ &= AF_{\boldsymbol{s}_{k_1}, \boldsymbol{s}_{k_2}}(\tau, f) \sum_{m=0}^{M-1} \xi_N^{-\tau d_m}. \end{aligned} \tag{55}$$

Next, we continue the discussion into two cases: (1) For $\tau \ne 0$, then $\max\left|AF_{\boldsymbol{C}^{(k_1)}, \boldsymbol{C}^{(k_2)}}(\tau, f)\right| = \alpha_{\max}\sqrt{\frac{M(N-M)}{N-1}}$. (2) For $\tau = 0$, then $\max\left|AF_{\boldsymbol{C}^{(k_1)}, \boldsymbol{C}^{(k_2)}}(\tau, f)\right| = M \times \max|AF_{\boldsymbol{s}_{k_1}, \boldsymbol{s}_{k_2}}(0, f)|$. When $k_1 = k_2$, since $f \ne 0$, then $\max|AF_{\boldsymbol{s}_{k_1}, \boldsymbol{s}_{k_2}}(0, f)| = 0$. This means $\max|AF_{\boldsymbol{s}_{k_1}, \boldsymbol{s}_{k_2}}(0, f)| = \max\limits_{k_1 \ne k_2}|AF_{\boldsymbol{s}_{k_1}, \boldsymbol{s}_{k_2}}(0, f)|$. This completes the proof. □

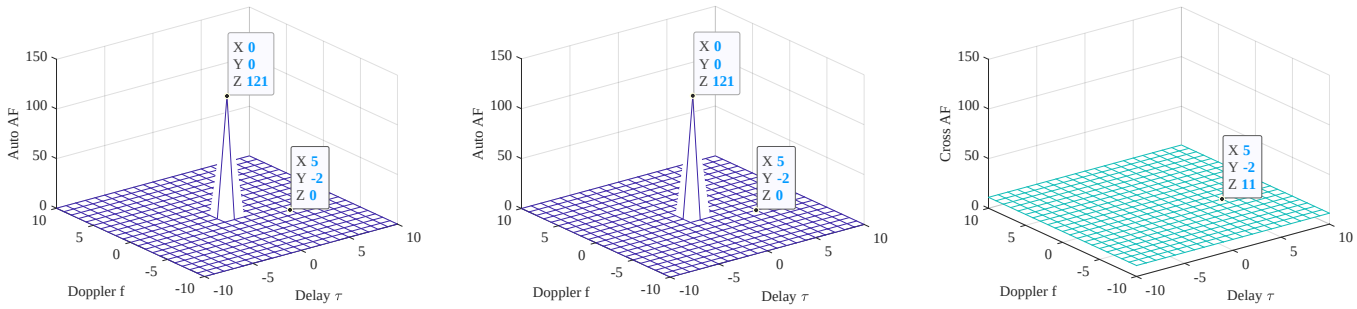

(a) Auto-AF of $\boldsymbol{C}^{(0)}$ (b) Auto-AF of $\boldsymbol{C}^{(5)}$ (c) Cross-AF of $\boldsymbol{C}^{(0)}$ and $\boldsymbol{C}^{(5)}$

Fig. 1: Periodic ambiguity functions of $\boldsymbol{C}^{(0)}$ and $\boldsymbol{C}^{(5)}$ in Example 2.

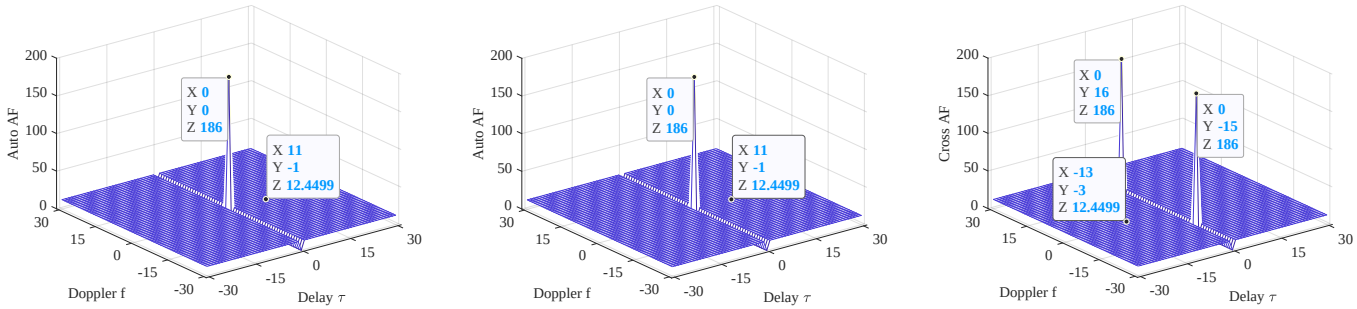

(a) Auto-AF of $\boldsymbol{C}^{(0)}$ (b) Auto-AF of $\boldsymbol{C}^{(1)}$ (c) Cross-AF of $\boldsymbol{C}^{(0)}$ and $\boldsymbol{C}^{(1)}$

Fig. 2: Periodic ambiguity functions of $\boldsymbol{C}^{(0)}$ and $\boldsymbol{C}^{(1)}$ in Example 3.

Lemma 8. Let N be an odd prime and $2 \leq K \leq N$. Define $\boldsymbol{S} = \{\boldsymbol{s}_k : 0 \leq k \leq K-1\}$, where $\boldsymbol{s}_k = (s_{k,0}, s_{k,1}, \cdots, s_{k,N-1})$, and

$$s_{k,n} = \xi_N^{n^3+k\lfloor N/K \rfloor n}. \tag{56}$$

Then $\boldsymbol{S}$ is a DRS set with maximum periodic ambiguity magnitude $\alpha_{\max} = \sqrt{N}$ and $\Pi = (-N+1, N-1) \times (-\lfloor N/K \rfloor, \lfloor N/K \rfloor)$.

Corollary 4. Let $N = 2^n - 1$ be a Mersenne prime, $\mathfrak{D}$ be a difference set of parameters (N, M, λ), and $\boldsymbol{S}$ be a LAZ sequence set obtained based on Lemma 8, where $n \geq 2$. Then $\mathcal{C}$ obtained through Theorem 8 is a asymptotically optimal with respect to the ambiguity lower bound in (16).

Proof. When $\tau = 0$, $AF_{\boldsymbol{s}_{k_1}, \boldsymbol{s}_{k_2}}(0, f) = 0$ for $f \in (-\lfloor N/K \rfloor, \lfloor N/K \rfloor)$. Therefore, the maximum periodic ambiguity magnitude $\theta_{\max}$ of $\mathcal{C}$ is $\theta_1 = \alpha_{\max}\sqrt{M(N-M)/(N-1)}$. According to Corollary 4, $Z_x = N$, $Z_y = \lfloor N/K \rfloor$. When $N \to \infty$, the optimal factor ρ of the DRCS set $\mathcal{C}$ is

$$\rho = \frac{\sqrt{\frac{NM(N-M)}{N-1}}}{\frac{MN}{\sqrt{Z_y}}\sqrt{\frac{KZ_xZ_y}{MN}-1}\over{KZ_x-1}} \approx \sqrt{1+\frac{N-Z_y}{N(N-1)}} = 1, \tag{57}$$

which indicates that $\mathcal{C}$ is asymptotically optimal. □

Example 3. Let $N = 2^5 - 1 = 31$, $K = 2$, $\mathfrak{D} = \{0, 1, 6, 18, 22, 29\}$ be a $(31, 6, 1)$-DS. According to Lemma 8, define

$$s_{0,n} = \xi_N^{n^3} \text{ and } s_{1,n} = \xi_N^{n^3+15n}, \tag{58}$$

where $0 \leq n \leq 30$. Based on $\{\boldsymbol{s}_0, \boldsymbol{s}_1\}$ and Corollary 4, we obtained a $(2, 6, 31, 12.45, \Pi)$-DRCS set $\mathcal{C} = \{\boldsymbol{C}^{(0)}, \boldsymbol{C}^{(1)}\}$, where $\Pi = (-31, 31) \times (-15, 15)$, the magnitudes of ambiguity function value of DRCS $\boldsymbol{C}^{(0)}$ and $\boldsymbol{C}^{(1)}$ are presented in Fig 2.

Consider a difference set $\mathfrak{D}$ of parameters $(N = 2^n - 1, M = 2^{n-1} - 1, \lambda = 2^{n-2} - 1)$. Based on the Corollary 4, the optimal DRCS set can be generated. Table III lists the changes in the optimal factor when the parameters K and N change.

TABLE III: The optimal factor of DRCS sets generated by Corollary 4

ρ / K \ N	$N = 2^3 - 1$	$N = 2^5 - 1$	$N = 2^7 - 1$	$N = 2^{13} - 1$	$N = 2^{17} - 1$
$K = 2$	1.1127	1.0244	1.0059	1.0001	1.0000
$K = 3$	1.1269	1.0272	1.0066	1.0001	1.0000
$K = 4$	-	1.0675	1.0151	1.0002	1.0000
$K = 5$	-	1.0295	1.0112	1.0001	1.0000

V. Application of DRCSs in Pulse Train Waveform

The application of DRCSs in engineering can be achieved through frequency division multiplexing or time-division multiplexing. Below we will briefly introduce an example of time-division multiplexing (i.e., pulse train waveform). Prior to that, we provide a concise introduction to the concept of phase encoding waveforms.

Let $\Omega(t)$ be a unit energy pulse shaping waveform with a duration of T_c, i.e., $\int_{-T_c/2}^{T_c/2} |\Omega(t)|^2 \mathrm{d}t = 1$. A baseband

waveform constructed by phase coding of $\Omega(t)$, with a length-N unimodular sequence $\boldsymbol{z} = (z_0, z_1, \cdots, z_{N-1})$ can be expressed as

$$z(t) = \sum_{n=0}^{N-1} z_n \Omega(t - nT_c). \tag{59}$$

Consider a coherent processing interval (CPI) containing M pulses, and the m-th pulse waveform $z_m(t)$ is obtained by length-N sequence $\boldsymbol{z}_m = (z_{m,0}, z_{m,1}, \cdots, z_{m,N-1})$ through phase coding technology, and the pulse repetition interval (PRI) is T_{pri}. Further, the pulse train waveform can be expressed as

$$u(t) = \sum_{m=0}^{M-1} z_m(t - mT_{\text{pri}}). \tag{60}$$

Without loss of generality, let us assume that the distance of detection targets does not exceed the maximum unambiguous distance. The discrete AF of $u(t)$ can be represented as

$$\chi_u(\tau, f_d) = \sum_{m=0}^{M-1} \sum_{n=0}^{N-1-\tau} z_{m,n} z_{m,n+\tau}^* \times \exp(j2\pi f_d(nT_c + mT_{\text{pri}})). \tag{61}$$

In [7], Pezeshki *et al.* assume $T_{\text{pulse}} = NT_c \ll T_{\text{pri}}$ (or $f_d \ll 1/T_{\text{pri}}$). Therefore (61) becomes

$$\chi_u(\tau, \theta) \approx \sum_{m=0}^{M-1} \tilde{R}_{\boldsymbol{z}_m}(\tau) e^{jm\theta}, \tag{62}$$

where $\theta = 2\pi f_d T_{\text{pri}}$, $\tilde{R}_{\boldsymbol{z}}(\tau) = \widetilde{AF}_{\boldsymbol{z}}(\tau, 0)$ denotes the aperiodic auto-correlation function of sequence $\boldsymbol{z}$. One possible solution is to design perfect sequences with zero aperiodic auto-correlation sidelobes [42]. Since this is challenging in general, Pezeshki *et al.* proposed DRGCWs based on GCP and PTM sequences. The special combination structure of a PTM sequence allows the Taylor expansion of $\chi_u(\tau, \theta)$ at $\theta = 0$ has high-order zeros, thus giving rise to Doppler resilience.

In practice, the assumption $T_{\text{pulse}} \ll T_{\text{pri}}$ (or $f_d \ll 1/T_{\text{pri}}$) does not always hold, which may severely affect the performance of DRGCWs. Here, we consider $T_{\text{pri}} = xT_{\text{pulse}}$ and $f_d = f\Delta f$, where $\Delta f = B/N$ is Doppler resolution [43], $B = 1/T_c$ is bandwidth, $x \geq 1$ and $1 - N \leq f \leq N - 1$ are two integers. Therefore, (61) can be represented as

$$\chi_u(\tau, f) = \sum_{m=0}^{M-1} \widetilde{AF}_{\boldsymbol{z}_m}(\tau, f). \tag{63}$$

At the receiver, the waveform processing flow is shown in Fig. 3.

TABLE IV: The delay and Doppler of 5 targets for integer f

No.	Delay	Doppler	RCS
1	$200 \times T_c = 0.1$ ms	$0 \times \Delta f = 0$ Hz (0 m/s)	0.8 m^2
2	$600 \times T_c = 0.3$ ms	$4 \times \Delta f = 3096.2$ Hz (195.3 m/s)	0.4 m^2
3	$600 \times T_c = 0.3$ ms	$10 \times \Delta f = 9765.6$ Hz (488.3 m/s)	0.4 m^2
4	$200 \times T_c = 0.1$ ms	$-4 \times \Delta f = -3096.2$ Hz (-195.3 m/s)	0.8 m^2
5	$800 \times T_c = 0.4$ ms	$-6 \times \Delta f = -5859.4$ Hz (-293.0 m/s)	0.2 m^2

In the simulation, we consider DRCS length $N = 2048$, carrier frequency $f_c = 3$ GHz, bandwidth $B = 2$ MHz, chip duration $T_c = 500$ ns, Doppler resolution $\Delta f = 976.6$ Hz,

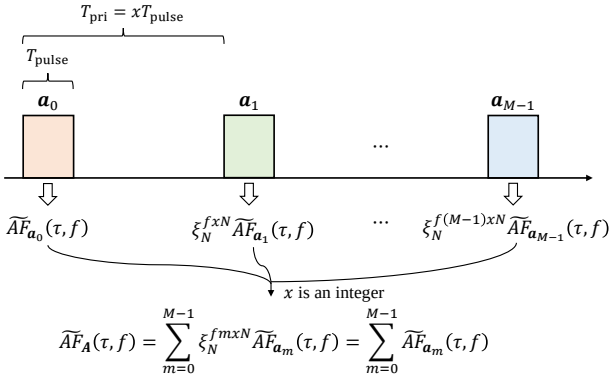

Fig. 3: Application of DRCSs in pulse train waveform, where $f_d = f \times \Delta f$ and f is an integer.

pulse duration $T_{\text{pulse}} = 1$ ms, PRI $T_{\text{pri}} = 10$ ms and number of pulses $M = 2048$. Let us consider 5 targets as shown in Table IV. We modeled these targets using the Swerling II model with model parameter $\sigma = 0.2$, which refers to the variance of the target Radar cross section (RCS) oscillation and by considering a signal-to-noise ratio (SNR) of -15 dB. In Fig. 4(a), we present the normalized delay-Doppler radar map after passing through a matched filter bank. From Fig. 4(a), we can see that the five targets listed in Table IV can be clearly reflected on the delay-Doppler map. Due to the excellent AF properties of DRCSs, the sidelobes in the delay-Doppler map are also very low (all are less than -30 dB), which has a relatively small impact on radar detection. As a comparison, we also provide the delay-Doppler map of DRGCWs, as shown in Fig. 4(b). By observation, the five targets can also be reflected in the delay-Doppler map of DRGCWs, but there are a large number of high sidelobes, and the maximum sidelobe is -12.6 dB. This may significantly impact the detection of target 5, given its normalized amplitude of -14.0 dB. To understand the poor performance of DRGCWs, we can explain from the following perspectives:

- Firstly, in the simulation, assuming $T_{\text{pri}} = 10$ ms, but $T_{\text{pri}} = 1$ ms, which cannot satisfy the constraint of $T_{\text{pulse}} \ll T_{\text{pri}}$;
- Secondly, the Doppler shift of the targets in the scenario is relatively large, which does not meet $f_d \ll 1/T_{\text{pri}}$;
- Thirdly, DRGCW inherently exhibits Doppler resilience, primarily around the zero Doppler axis, limiting its effectiveness with large Doppler shifts.

In the above simulation, we utilized DRCS with length $N = 2048$ to achieve a Doppler resolution of $\Delta f = 976.6$ Hz. For short DRCS, the Doppler resolution may become very poor. For example, if we take $N = 64$, the Doppler resolution then is $\Delta f = B/N = 31.25$ kHz, and the corresponding velocity resolution is $\Delta v = 1562.5$ m/s, which is not friendly for the velocity detection of moving targets. In this case, we can adopt the waveform transmission and processing method shown in Fig. 5, where "MF" is the abbreviation of matched filter. Below, we give a simulation example. Here, we consider DRCS length $N = 64$, carrier frequency $f_c = 3$ GHz, bandwidth $B = 2$ MHz, chip duration $T_c = 500$ ns,

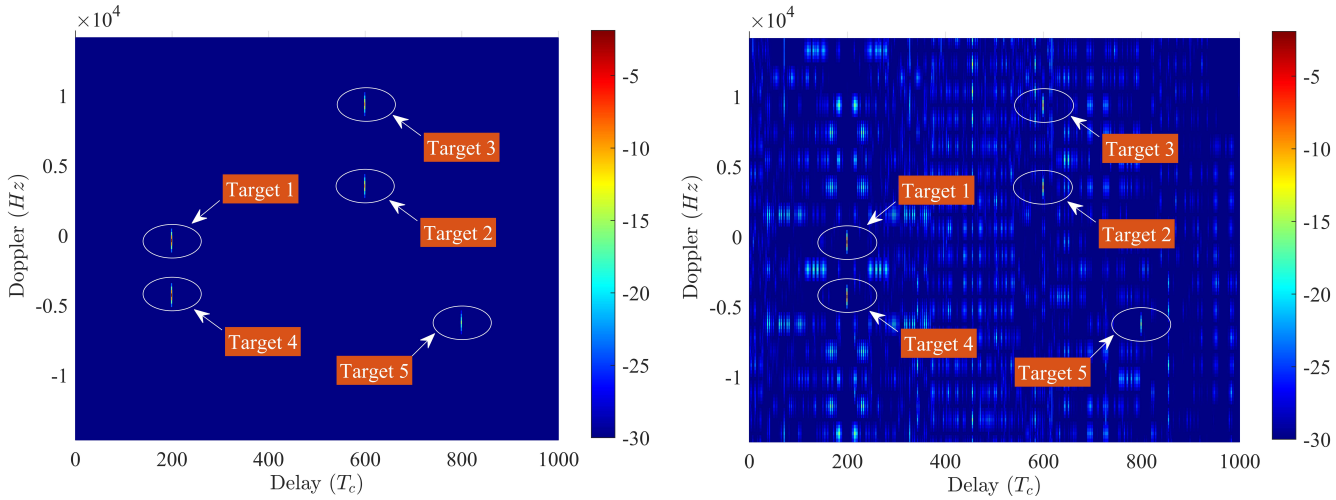

(a) DRCS-Based (b) DRGCW [7]

Fig. 4: Normalized multi-target delay-Doppler map for integer f.

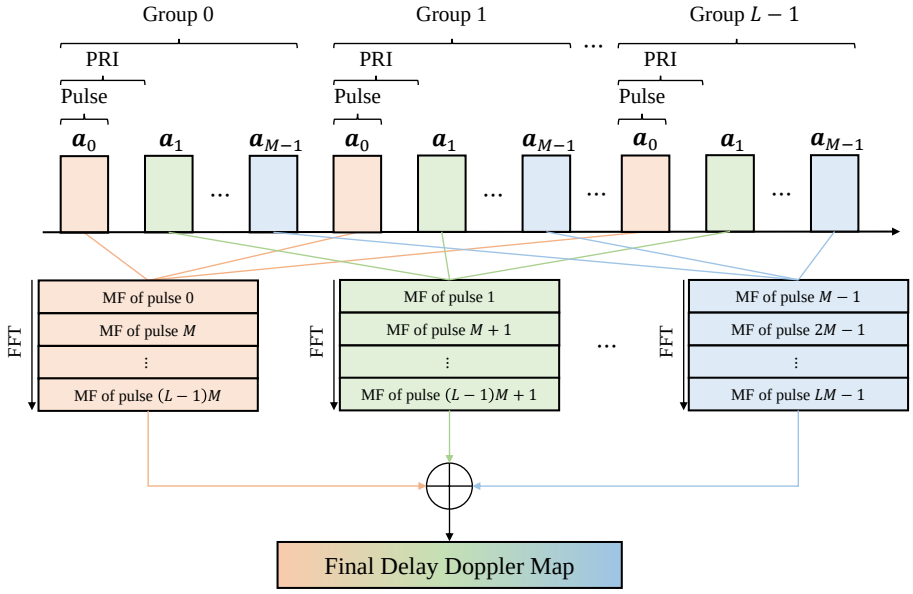

Fig. 5: Application of DRCSs in pulse train waveform, where $f_d = f \times \Delta f$ and f is a fraction.

$\Delta f = B/N = 31.25$ kHz, pulse duration $T_{\text{pulse}} = 62$ μs, PRI $T_{\text{pri}} = 620$ μs and number of pulses $M' = 128 \times 64 = 8192$.

TABLE V: The delay and Doppler of 3 targets for fraction f

No.	Delay	Doppler	RCS
1	$200 \times T_c = 0.1$ ms	$0.02 \times \Delta f = 625.0$ Hz (31.250 m/s)	0.8 m^2
2	$400 \times T_c = 0.2$ ms	$0.01 \times \Delta f = 312.5$ Hz (15.625 m/s)	0.4 m^2
3	$400 \times T_c = 0.2$ ms	$0.02 \times \Delta f = 625.0$ Hz (31.250 m/s)	0.4 m^2

In this scenario, we consider 3 targets as shown in Table V. Similarly, we modeled the targets using the Swerling II model with model parameter $\sigma = 0.2$ and considering a SNR of -15 dB. In Fig. 6, we provide the normalized delay-Doppler radar map. From Fig. 6, we can see that the three targets listed in Table V can be clearly reflected on the delay-Doppler map. This shows that DRCSs can provide good target detection performance even for fractional f.

VI. Conclusion

This paper has introduced a new concept called DRCS aiming for attaining zero/low AF zone properties. Based on this new concept, three types of theoretical bounds on unimodular DRCS sets with respect to the set size, the flock size, the sequence length, and the zone size of low/zero ambiguity zone have been derived. Additionally, for aperiodic ambiguity functions, based on the upper bound of the number of CS sets with zero correlation zone, an upper bound on the number of DRCS sets with zero ambiguity zone has been derived. Then, based on the orthogonal matrix, the Florentine rectangle and the difference set, some types construction of DRCS sets have been proposed. These DRCS sets are proved to be optimal with respect to the derived lower bounds, as shown in Table VI. Finally, we have introduced the application of DRCS in the waveform design of pulse train radar and verified the

TABLE VI: Parameters of the proposed DRCS set

Source	Parameters	Type	Notes
Theorem 5	(N, N)	aperiodic periodic odd-periodic	perfect DRCS based on order-N Fourier matrix and random sequence
Theorem 6	(P, PN, N)	aperiodic periodic odd-periodic	perfect DRCS set based on order-N Fourier matrix and order-P orthogonal matrix
Theorem 7	(K, N, N, N)	periodic	optimal DRCS set based on CFR of size $K \times N$
Corollary 3	(K, N, N, N)	aperiodic	near-optimal DRCS set based on FR of size $K \times N$
Theorem 8	$(K, M, N, \theta_{\max}, \Pi)$	periodic	DRCS set based on (N, M, λ)-DS and $(K, N, \alpha_{\max}, \Pi)$-DRS, where $\theta_{\max} = \max\left\{\alpha_{\max}\sqrt{\frac{M(N-M)}{N-1}}, M \cdot \max_{k_1 \neq k_2} \left|AF_{\boldsymbol{s}_{k_1}, \boldsymbol{s}_{k_2}}(0, f)\right|\right\}$
Corollary 4	$\left(K, M, N, \sqrt{\frac{NM(N-M)}{N-1}}, \Pi\right)$	periodic	optimal DRCS set from Theorem 8, where $N = 2^n - 1$ is a prime and $\Pi = (-N+1, N-1) \times (-\lfloor N/K \rfloor, \lfloor N/K \rfloor)$

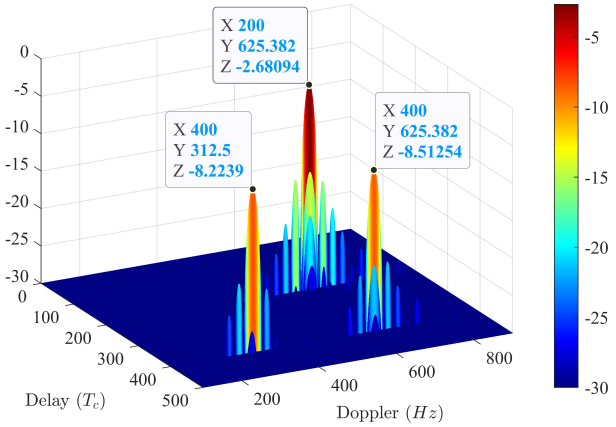

Fig. 6: Normalized multi-target delay-Doppler map for fraction f.

practicality of DRCS based waveforms through simulation. In the future, it would be interesting, albeit more challenging, to explore tighter aperiodic ambiguity lower bounds and the corresponding optimal DRCS constructions.

ACKNOWLEDGMENTS

The authors are very grateful to the editor, Prof. Lilya Budaghyan, and the anonymous reviewers for their valuable comments and suggestions that improved the quality of this paper.

REFERENCES

[1] M. Golay, "Complementary series," *IRE Transactions on Information Theory*, vol. 7, no. 2, pp. 82–87, 1961.
[2] C.-C. Tseng and C. Liu, "Complementary sets of sequences," *IEEE Transactions on Information Theory*, vol. 18, no. 5, pp. 644–652, 1972.
[3] N. Suehiro and M. Hatori, "N-shift cross-orthogonal sequences," *IEEE Transactions on Information Theory*, vol. 34, no. 1, pp. 143–146, 1988.
[4] L. Bomer and M. Antweiler, "Periodic complementary binary sequences," *IEEE Transactions on Information Theory*, vol. 36, no. 6, pp. 1487–1494, 1990.
[5] H. D. Luke, "Binary odd-periodic complementary sequences," *IEEE Transactions on Information Theory*, vol. 43, no. 1, pp. 365–367, 1997.
[6] P. Spasojevic and C. N. Georghiades, "Complementary sequences for ISI channel estimation," *IEEE Transactions on Information Theory*, vol. 47, no. 3, pp. 1145–1152, 2001.
[7] A. Pezeshki, A. R. Calderbank, W. Moran, and S. D. Howard, "Doppler resilient Golay complementary waveforms," *IEEE Transactions on Information Theory*, vol. 54, no. 9, pp. 4254–4266, 2008.
[8] Q. Wang, H. Yang, L. Wu, L. Zhang, Y. Xia, X. Fu, and C. Tan, "Complementary coding-based waveform design for broadband acoustic doppler current profilers," *IEEE Transactions on Vehicular Technology*, 2024.
[9] D. Su, Y. Jiang, X. Wang, and X. Gao, "Omnidirectional precoding for massive MIMO with uniform rectangular array—Part I: Complementary codes-based schemes," *IEEE Transactions on Signal Processing*, vol. 67, no. 18, pp. 4761–4771, 2019.
[10] N. Y. Yu, "Binary Golay spreading sequences and Reed-Muller codes for uplink grant-free NOMA," *IEEE Transactions on Communications*, vol. 69, no. 1, pp. 276–290, 2020.
[11] H.-H. Chen, J.-F. Yeh, and N. Suehiro, "A multicarrier CDMA architecture based on orthogonal complementary codes for new generations of wideband wireless communications," *IEEE Communications Magazine*, vol. 39, no. 10, pp. 126–135, 2001.
[12] Z. Liu, Y. L. Guan, and H.-H. Chen, "Fractional-delay-resilient receiver design for interference-free MC-CDMA communications based on complete complementary codes," *IEEE transactions on Wireless Communications*, vol. 14, no. 3, pp. 1226–1236, 2015.
[13] A. Şahin, "Encoding and decoding with partitioned complementary sequences for Low-PAPR OFDM," *IEEE Transactions on Wireless Communications*, vol. 21, no. 4, pp. 2561–2572, 2021.
[14] P. Kumari, J. Choi, N. González-Prelcic, and R. W. Heath, "IEEE 802.11 ad-based radar: An approach to joint vehicular communication-radar system," *IEEE Transactions on Vehicular Technology*, vol. 67, no. 4, pp. 3012–3027, 2017.
[15] G. Duggal, S. Vishwakarma, K. V. Mishra, and S. S. Ram, "Doppler-resilient 802.11 ad-based ultrashort range automotive joint radar-communications system," *IEEE Transactions on Aerospace and Electronic Systems*, vol. 56, no. 5, pp. 4035–4048, 2020.
[16] Z. Liu, Y. Guan, B. C. Ng, and H.-H. Chen, "Correlation and set size bounds of complementary sequences with low correlation zone," *IEEE Transactions on Communications*, vol. 59, no. 12, pp. 3285–3289, 2011.
[17] L. Welch, "Lower bounds on the maximum cross correlation of signals (corresp.)," *IEEE Transactions on Information theory*, vol. 20, no. 3, pp. 397–399, 1974.
[18] Z. Liu, Y. L. Guan, and W. H. Mow, "A tighter correlation lower bound for quasi-complementary sequence sets," *IEEE Transactions on Information Theory*, vol. 60, no. 1, pp. 388–396, 2014.
[19] Z. Liu, U. Parampalli, Y. L. Guan, and S. Boztas, "Constructions of optimal and near-optimal quasi-complementary sequence sets from singer difference sets," *IEEE Wireless Communications Letters*, vol. 2, no. 5, pp. 487–490, 2013.
[20] Y. Li, L. Tian, T. Liu, and C. Xu, "Constructions of quasi-complementary sequence sets associated with characters," *IEEE Transactions on Information Theory*, vol. 65, no. 7, pp. 4597–4608, 2019.
[21] G. Luo, X. Cao, M. Shi, and T. Helleseth, "Three new constructions of asymptotically optimal periodic quasi-complementary sequence sets with small alphabet sizes," *IEEE Transactions on Information Theory*, vol. 67, no. 8, pp. 5168–5177, 2021.
[22] T. Liu, C. Xu, and Y. Li, "Binary complementary sequence set with low correlation zone," *IEEE Signal Processing Letters*, vol. 27, pp. 1550–1554, 2020.
[23] A. R. Adhikary, Y. Feng, Z. Zhou, and P. Fan, "Asymptotically optimal and near-optimal aperiodic quasi-complementary sequence sets based on florentine rectangles," *IEEE Transactions on Communications*, vol. 70, no. 3, pp. 1475–1485, 2022.

[24] P. Sarkar, C. Li, S. Majhi, and Z. Liu, "New correlation bound and construction of quasi-complementary sequence sets," *IEEE Transactions on Information Theory*, vol. 70, no. 3, pp. 2201–2223, 2024.
[25] Z. Ye, Z. Zhou, P. Fan, Z. Liu, X. Lei, and X. Tang, "Low ambiguity zone: Theoretical bounds and doppler-resilient sequence design in integrated sensing and communication systems," *IEEE Journal on Selected Areas in Communications*, vol. 40, no. 6, pp. 1809–1822, 2022.
[26] C. Ding, K. Feng, R. Feng, M. Xiong, and A. Zhang, "Unit time-phase signal sets: Bounds and constructions," *Cryptography and Communications*, vol. 5, pp. 209–227, 2013.
[27] S. Li, "The ambiguity function analysis of complete complementary sequence in MIMO system," in *IEEE International Conference on Signal Processing, Communications and Computing*, 2015, pp. 1–5.
[28] J. Tang, N. Zhang, Z. Ma, and B. Tang, "Construction of Doppler resilient complete complementary code in MIMO radar," *IEEE Transactions on Signal Processing*, vol. 62, no. 18, pp. 4704–4712, 2014.
[29] W. Dang, A. Pezeshki, S. Howard, W. Moran, and R. Calderbank, "Coordinating complementary waveforms for sidelobe suppression," in *2011 Confer'ence Record of the Forty Fifth Asilomar Conference on Signals, Systems and Computers*, 2011, pp. 2096–2100.
[30] J. Zhu, X. Wang, X. Huang, S. Suvorova, and B. Moran, "Range sidelobe suppression for using Golay complementary waveforms in multiple moving target detection," *Signal Processing*, vol. 141, pp. 28–31, 2017.
[31] J. Zhu, N. Chu, Y. Song, S. Yi, X. Wang, X. Huang, and B. Moran, "Alternative signal processing of complementary waveform returns for range sidelobe suppression," *Signal Processing*, vol. 159, pp. 187–192, 2019.
[32] F. Wang, C. Pang, H. Wu, Y. Li, and X. Wang, "Designing constant modulus complete complementary sequence with high doppler tolerance for simultaneous polarimetric radar," *IEEE Signal Processing Letters*, vol. 26, no. 12, pp. 1837–1841, 2019.
[33] Z.-J. Wu, C.-X. Wang, P.-H. Jiang, and Z.-Q. Zhou, "Range-doppler sidelobe suppression for pulsed radar based on golay complementary codes," *IEEE Signal Processing Letters*, vol. 27, pp. 1205–1209, 2020.
[34] J. Wang, P. Fan, Z. Zhou, and Y. Yang, "Quasi-orthogonal z-complementary pairs and their applications in fully polarimetric radar systems," *IEEE Transactions on Information Theory*, vol. 67, no. 7, pp. 4876–4890, 2021.
[35] G. Duggal, S. Vishwakarma, K. V. Mishra, and S. S. Ram, "Doppler-resilient 802.11 ad-based ultrashort range automotive joint radar-communications system," *IEEE Transactions on Aerospace and Electronic Systems*, vol. 56, no. 5, pp. 4035–4048, 2020.
[36] R. Turyn, "Ambiguity functions of complementary sequences (corresp.)," *IEEE Transactions on Information Theory*, vol. 9, no. 1, pp. 46–47, 1963.
[37] H. Y. Song, "On aspects of tuscan squares," Ph.D. dissertation, Department of Electrical Engineering, University of Southern California, Los Angeles, CA, USA, 1991.
[38] D. Sarwate, "Bounds on crosscorrelation and autocorrelation of sequences (Corresp.)," *IEEE Transactions on Information Theory*, vol. 25, no. 6, pp. 720–724, 1979.
[39] M. Pursley, "Performance evaluation for phase-coded spread-spectrum multiple-access communication-Part II: code sequence analysis," *IEEE Transactions on Communications*, vol. 25, pp. 800–803, 1977.
[40] W. H. Mow, "Even-odd transformation with application to multiuser CW radars," *IEEE Transactions on Aerospace and Electronic Systems*, vol. 35, no. 4, pp. 1466–1470, 1999.
[41] P. Fan, W. Yuan, and Y. Tu, "Z-complementary binary sequences," *IEEE Signal Processing Letters*, vol. 14, no. 8, pp. 509–512, 2007.
[42] J. Wang, P. Fan, Q. Shi, and Z. Zhou, "Doppler resilient integrated sensing and communication waveforms design," *Journal of Radars*, vol. 12, no. 2, pp. 275–286, 2023.
[43] X. Liu, Y. L. Guan, R. Jagannath, Y. Lu, J. Wang, and P. Fan, "Joint radar communication with novel GCC preamble and point-wise minimum fusion," *IEEE Transactions on Vehicular Technology*, vol. 72, no. 3, pp. 3321–3334, 2022.

Bingsheng Shen (Member, IEEE) received the B.S. and Ph.D degrees in Chengdu University (CDU), Chengdu, China, in 2018, and in Southwest Jiaotong University (SWJTU), Chengdu, China in 2023, respectively. Since 2023, he has been in the School of Information Science and Technology, Southwest Jiaotong University, where he is currently an associate researcher. His research topic concentrates on sequence design in modern communication systems and radar.

Yang Yang (Member, IEEE) received the B.S. and M.S. degrees in Hubei University, Wuhan, China, in 2005 and 2008, respectively and the Ph.D. degree in Southwest Jiaotong University, Chengdu, China in 2012. Since 2013, he has been in the School of Mathematics, Southwest Jiaotong University, where he is currently a professor. His research interests include applied mathematics, sequence design and its applications, integrated signal for radar and communication.

Zhengchun Zhou (Member, IEEE) received the B.S. and M.S. degrees in mathematics and the Ph.D. degree in information security from Southwest Jiaotong University, Chengdu, China, in 2001, 2004, and 2010, respectively. From 2012 to 2013, he was a postdoctoral member in the Department of Computer Science and Engineering, the Hong Kong University of Science and Technology. From 2013 to 2014, he was a research associate in the Department of Computer Science and Engineering, the Hong Kong University of Science and Technology. Since 2004, he has been in Southwest Jiaotong University, where he is currently a professor. His research interests include sequence design, Boolean function, coding theory, and compressed sensing. He is an associated editor of IEEE Transactions on Cognitive Communications and Networking, Advances in Mathematics of Communications and IEICE Transactions on Fundamentals, and was a Guest Editor for special issues of Cryptography and Communications. Dr. Zhou was the recipient of the National excellent Doctoral Dissertation award in 2013 (China).

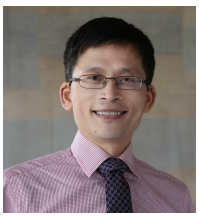

Zilong Liu (Senior Member, IEEE) is an Associate Professor and the 6G Lab Manager with the School of Computer Science and Electronic Engineering, University of Essex. His research generally lies in the interplay of coding, signal processing, and communications, with a major objective of bridging theory and practice. His recent research interests include advanced 6G V2X communication, sensing, and localization technologies for future connected autonomous vehicles as well as machine learning for enhanced communications and networking.

He received his PhD (2014) from School of Electrical and Electronic Engineering, Nanyang Technological University (NTU, Singapore), advised by Prof Yong Liang Guan, Master Degree (2007) in the Department of Electronic Engineering from Tsinghua University (China), advised by Prof Huazhong Yang (IEEE Fellow), and Bachelor Degree (2004) in the School of Electronics and Information Engineering from Huazhong University of Science and Technology (HUST, China). He was also a Visiting PhD student to Hong Kong University of Science and Technology (HKUST, hosted by Prof Wai Ho Mow) and the University of Melbourne (hosted by Prof Udaya Parampalli). From Jan. 2018 to Nov. 2019, he was a Senior Research Fellow at the Institute for Communication Systems (ICS), Home of the 5G Innovation Centre (5GIC), University of Surrey, during which he studied the air-interface design of 5G communication networks. Prior to his career in UK, he spent nine and half years in NTU, first as a Research Associate (Jul. 2008 to Oct. 2014) and then a Research Fellow (Nov. 2014 to Dec. 2017). His PhD thesis "Perfect- and Quasi- Complementary Sequences", focusing on fundamental limits, algebraic constructions, and applications of complementary sequences in wireless communications, has settled a few long-standing open problems in the field. He is a Senior Member of IEEE and an Associate Editor of IEEE Transactions on Wireless Communications, IEEE Transactions on Vehicular Technology, IEEE Transactions on Neural Networks and Learning Systems, IEEE Wireless Communications Letters, IEEE Open Journal of the Communication Society, and Advances in Mathematics of Communications. He was the Hosting General Chair of the 12th Sequences and Their Applications (SETA'2024, https://seta-2024.github.io/) and the 10th IEEE International Workshop on Signal Design and its Applications in Communications (iwsda2022.github.io). He was named the 2024 Outstanding Mid-Career Researcher in the Faculty of Science and Health, the University of Essex. He was a Red Bird Visiting Scholar in HKUST from December 2023 to January 2024. He was a Consultant to the Japanese government on 6G assisted autonomous driving in January 2023. He is/was the Leading Track Chair on Signal Processing for Wireless Communications in IEEE VTC2025-Fall. He was a Track Co-Chair on Networking and MAC in IEEE PIMRC'2023. Details of his research can be found at: https://sites.google.com/site/zilongliu2357.

Pingzhi Fan (Life Fellow, IEEE) received the M.Sc. degree in computer science from Southwest Jiaotong University (SWJTU), China, in 1987, and the Ph.D. degree in electronic engineering from Hull University, U.K., in 1994. He is currently a Presidential Professor with SWJTU, the Honorary Dean of the SWJTU-Leeds Joint School, and has been a Visiting Professor with Leeds University, U.K., since 1997. His research interests include high mobility wireless communications, massive random-access techniques, and signal design and coding. He is an IEEE VTS Distinguished Speaker (2019–2025); and a fellow of IET, CIE, and CIC. He served as an EXCOM Memberfor the IEEE Region 10, IET (IEE) Council, and the IET Asia-Pacific Region. He was a recipient of U.K. ORS Award in 1992, the National Science Fund for Distinguished Young Scholars in 1998 (NSFC), IEEE VT Society Jack Neubauer Memorial Award in 2018, IEEE SP Society SPL Best Paper Award in 2018, IEEE/CIC ICCC2020 Best Paper Award, IEEE WCSP2022 Best Paper Award, and IEEE ICC2023 Best Paper Award. He served as a Chief Scientist for the National 973 Plan Project (National Basic Research Program of China) between January 2012 and December 2016.